Supporting Information

Kershner et al. 10.1073/pnas.1401861111

SI Materials and Methods

Nematode Culture. Strains were maintained at 20 °C following standard protocols (1), except for H2B::GFP reporter transgenic lines which were maintained at 25 °C. Wild type was the N2 Bristol strain. Mutations were as follows: *LG I*: *gld-1(q485)* (2); *gld-2(q497)* (3); *lst-1(ok814)* (4); *sygl-1(tm5040)* (this work); *rrf-1 (pk1417)* (5); *LG II*: *fbf-1(ok91)* (6); *fbf-2(q704)* (6); *fbf-2(q738)* (7); *LG III*: *glp-1(q46)* (8); *glp-1(oz112 gf)* (9); *LG IV*: *lip-1(zh15)* (10); *eri-1(mg366)* (11). *lst-1(ok814)* and *sygl-1(tm5040)* single mutants were outcrossed against wild type at least eight times before analysis. Balancers were as follows: *LG I*: *hT2[qIs48]* (12); *LG II*: *mIn1[mIs14 dpy-10(e128)]*; *LG III*: *hT2[qIs48]*; *qC1 [qIs26]*. Transgenes were as follow: *LG II*: *qSi26[$P_{sygl\text{-}1(wt)}$::H2B::GFP::sygl-1 3′end; unc-119(+)]* (this study); *qSi29[$P_{sygl\text{-}1(4XLBS\ mut)}$::H2B::GFP::sygl-1 3′end; unc-119(+)]* (this work); *LG III*: *qIs153[$P_{lag\text{-}2}$::MYR::GFP; $P_{ttx\text{-}3}$::DsRED]* (13); *LG IV: teIs1 [oma-1::GFP; unc-119(+)]* (14); unknown *LG*: *qIs147[Psur-5::GFP]*.

Nematode Strains Used in This Study. The nematode strains used in this study were as follows:

N2: wild-type

GR1373: *eri-1(mg366) IV*

NL2098: *rrf-1(pk1417) I*

EG4322: *ttTi5605 II; unc-119(ed3) III*

JK2879: *gld-2(q497) gld-1(q485) I/ hT2[qIs48](I;III)*

JK3308: *fbf-2(q738)/ mIn1[mIs14 dpy-10(e128)] II; lip-1(zh15) IV*

JK3520: *unc-32(e189) glp-1(oz112 gf)/ qC1[qIs26] III*

JK3545: *gld-2(q497) gld-1(q485) I/ hT2[qIs48](I;III); unc-32 (e189) glp-1(q46) III/ hT2[qIs48](I;III)*

JK3635: *fbf-1(ok91) fbf-2(q704)/ mIn1[mIs14 dpy-10(e128)] II*

JK4008: *fbf-1(ok91) fbf-2(q704)/ mIn1[mIs14 dpy-10(e128)] II; lip-1(zh15) IV*

JK4356: *lst-1(ok814) I*

JK4475: *qIs153[$P_{lag\text{-}2}$::MYR::GFP; $P_{ttx\text{-}3}$::DsRED] III*

JK4774: *lst-1(ok814) sygl-1(tm5040) I/ hT2[qIs48](I;III)*

JK4795: *lst-1(ok814) sygl-1(tm5040) I/ hT2[qIs48](I;III); qIs147 [$P_{sur\text{-}5}$::GFP] (LG?)*

JK4832: *gld-2(q497) gld-1(q485) lst-1(ok814) sygl-1(tm5040) I/ hT2[qIs48](I;III)*

JK4862: *glp-1(q46) III/ hT2[qIs48](I;III)*

JK4873: *gld-2(q497) gld-1(q485) I/ hT2[qIs48](I;III); unc-32 (e189) III/ hT2[qIs48](I;III)*

JK4899: *sygl-1(tm5040) I*

JK5017: *gld-2(q497) gld-1(q485) lst-1(ok814) sygl-1(tm5040) I/ hT2[qIs48](I;III); glp-1(q46) III/ hT2[qIs48](I;III)*

JK5018: *qSi26[$P_{sygl\text{-}1(wt)}$::H2B::GFP::sygl-1 3′end; unc-119(+)] II; unc-119(ed3) III; teIs1[oma-1::GFP, unc-119(+)] IV** (**teIs1* was crossed out before scoring)

JK5072: *qSi29[$P_{sygl\text{-}1(4XLBS\ mut)}$::H2B::GFP::sygl-1 3′end; unc-119(+)] II; unc-119(ed3) III; teIs1[oma-1::GFP; unc-119(+)] IV** (**teIs1* was crossed out before scoring)

Immunocytochemistry. Antibody staining of dissected gonads was carried out essentially as described (15). Briefly, dissected gonads were fixed in 3% (wt/vol) paraformaldehyde and 100 mM K_2HPO_4 (pH 7.2) for 0.5–1 h at room temperature and then permeabilized in 100% methanol at −20 °C for 10 min. Samples were washed three times in PBST (PBS plus 0.1% Tween-20) and blocked in PBST plus 0.5% BSA for 30 min at room temperature. Primary antibodies were incubated at 4 °C overnight at the following dilutions in PBST plus 0.5% BSA: the sperm marker mouse anti-SP56, 1:100 (16); the nucleolar marker mouse anti–DAO-5, 1:10 (17); the meiotic marker rabbit anti–HIM-3, 1:200 (18); the mitotic marker rabbit anti–REC-8, 1:5,000 (SDIX); and the germ cell marker rabbit anti–PGL-1, 1:100 (19). Cy5, Cy3, and FITC conjugated secondary antibodies (Jackson ImmunoResearch) were used at 1:500 dilution in PBST plus 0.5% BSA for 1–2 h at room temperature. 4′,6-diamidino-2-phenylindole (DAPI) (0.5 ng/μL) was included to visualize DNA. Compound microscope images were taken using a Zeiss Axioimager microscope, and confocal images were taken using a Leica TCS SP8.

Antibody staining of whole animals was carried out essentially as described (20). Briefly, animals were subjected to three rounds of freeze–thaw cycles in FRB [80 mM KCl, 20 mM NaCl, 10 mM EGTA, 5 mM spermidine, 15 mM Pipes (pH 7.4), 25% (vol/vol) methanol, 0.8% paraformaldehyde], followed by a 30-min fixation on ice. Fixed samples were washed twice in TT [100 mM Tris (pH 7.4), 1% Triton X-100, 1 mM EDTA] and then reduced for 4 h in TT plus 1% β-mercaptoethanol at 37 °C. Samples were then washed once in BO_3T [50 mM H_3BO_3 (pH 9.5), 25 mM NaOH, 0.01% Triton X-100] and incubated with BO_3T plus 10 mM DTT at room temperature for 15 min. Next, samples were washed once with BO_3T and then oxidized with BO_3T plus 0.3% H_2O_2 for 15 min at room temperature followed by two washes with PBST. Samples were blocked in PBST plus 0.5% BSA and stained using rabbit anti–PGL-1 antibodies (19) at a 1:100 dilution in PBST plus 0.5% BSA. FITC-conjugated anti-rabbit secondary antibodies (Jackson ImmunoResearch) were used at 1:500 dilution in PBST plus 0.5% BSA. DAPI (0.5 ng/μL) was included to visualize DNA. Samples were imaged using a Zeiss Axioimager microscope.

mRNA in Situ Hybridization. mRNA in situ hybridizations were carried out on dissected gonads from either adult hermaphrodites grown to 24 h post L4 stage or from L4 larva, as indicated in the figure legends for Fig. 3 and Fig. 4, following standard protocols (21). For probe generation, PCR fragments were amplified from cDNA using the following primers: *lst-1*, prAK102 (5′-ggcttcttcgtcggagaacatg-3′) and prAK104 (5′-gaaccggcacgatcgagttg-3′); *sygl-1*, prAK329 (5′-atgccattccattatccaaaactc-3′), and prAK330 (5′-atagctgttggagcccatcatc-3′). Fragments were occasionally subject to two rounds of PCR to generate more concentrated probe. Next, single-stranded digoxigenin (DIG)-dUTP labeled DNA probes were generated from the PCR fragments using DIG labeling mix (Roche) following the manufacturer's protocol with either antisense or sense primer as follows: *lst-1* sense, prAK105 (5′-gttgacgtggatcttgacat-3′); *lst-1* antisense, prAK101 (5′-gttgagcaaaccacagtcgg-3′); *sygl-1* sense, prAK331 (5′-ggaaacatgtccacctcatcgtc-3′); and *sygl-1* antisense, prAK332 (5′-ggtaactgtggagaccaaatcgg-3′). Probes were ethanol precipitated, resuspended in hybridization buffer (HB) [5× SSC, 50% (vol/vol) deionized formamide,

100 μg/mL herring sperm DNA, 50 μg/mL heparin, 0.1% Tween-20], and boiled for 1 h. To prepare worm samples, dissected gonads were fixed in 3% (wt/vol) paraformaldehyde, 0.25% glutaraldehyde, 100 mM K_2HPO_4 (pH 7.2) at room temperature for 2 h. Samples were then permeabilized in 100% (vol/vol) methanol at −20 °C and washed three times in PBST. Samples were then digested with 50 μg/mL Proteinase K in PBST for 30 min at room temperature and then fixed again using 3% (wt/vol) paraformaldehyde, 0.25% glutaraldehyde, 100 mM K_2HPO_4 (pH 7.2) at room temperature for 15 min. After a 15-min incubation with PBST plus 2 mg/mL glycine, fixed samples were washed three times with PBST. Gonads were then treated with a 1:1 mixture of PBST and HB for 5 min at 48 °C, followed by an incubation with 100% HB at 48 °C for 1 h. Boiled probes were then added to the samples and were incubated at 48 °C for 24–36 h. Next, samples were first washed 2–3 times in HB, then washed two to three times in a 1:1 mixture of PBST and HB, and then washed two to three times with PBST. For probe detection, samples were first blocked as above and then treated with anti-DIG antibody (Roche) diluted to 1:1,000 in PBST plus 0.5% BSA and incubated overnight at 4 °C. Samples were then washed two to three times with PBST plus 0.5% BSA and stained with BCIP/NBT substrate (Sigma) in 100 mM Tris (pH 9.5), 100 mM NaCl, 5 mM $MgCl_2$, 0.1% Tween-20, and 1 mM Levamisole. After staining appeared in the sample treated with antisense probe, samples were washed two to three times in PBST and then viewed using a Zeiss Axioskop microscope.

Transgenic *Caenorhabditis elegans*. For H2B::GFP reporter transgenes, a construct (pJK1634) containing ∼2.2 kb of sequence upstream of the *sygl-1* start driving expression of H2B::GFP coding sequence from pCM1.35 (Addgene; plasmid 17248) (22), followed by the *sygl-1* 3′UTR and intergenic region was cloned into the SpeI site of pCFJ151 (23) (Addgene; plasmid 19330). A separate clone (pJK1635) was generated identical to pJK1634 except that each of the four consensus LAG-1 binding sites was mutated from the wild-type consensus RTGGGAA to the mutant form RACGGAA using QuikChange Site Directed Mutagenesis Kit (Stratagene). pJK1634 and pJK1635 were then used to integrate the constructs into the *ttTi5605* site in *LGII* of strain EG4322 to make *qSi26* and *qSi29*, respectively, using *Mos1*-mediated single copy insertion (MosSCI) direct insertion method (23). Multiple transgenic lines generated for each construct showed similar expression patterns. Because *gfp* transgenes are often silenced in the germ line, each reporter was crossed into an *oma-1::gfp* germ line-expressing strain that can desilence other germline *gfp* transgenes in *trans* (24). Reporters were maintained for at least 10 generations in the *oma-1::gfp* background, after which they were crossed out and maintained at 25 °C. The presence of H2B::GFP was scored in unfixed tissues by dissecting gonads in PBST, 0.25 mM Levamisole, and Hoechst 33342 (Invitrogen) diluted 1:10,000, and visualized using the Zeiss Axioimager microscope. For both transgenic lines, H2B::GFP was observed in the proximal region of the germ line. Distal H2B::GFP was scored only in germ lines with proximal expression. Distal expression was never observed in the absence of proximal expression.

Northern Blots. Total RNA was extracted from staged N2, *lst-1(ok814)* (JK4356), and *sygl-1(tm5040)* (JK4899) adults grown to 24 h past L4 stage using TRIzol Reagent (Invitrogen). RNA was then poly(A) selected using the poly(A) Purist Kit (Ambion), and 5 μg of poly(A) RNA was run in each lane on a 1% or 1.2% (wt/vol) agarose gel under denaturing conditions using the NorthernMax-Gly kit (Ambion). RNA Millennium Markers (Ambion) were also run as a size marker. Separated RNA was transferred to a positively charged nylon membrane (BrightStar-Plus; Ambion) using NorthernMax transfer buffer (Ambion) and transferred RNA was then crosslinked to the membrane using Stratalinker UV cross-linker (Stratagene). In vitro-transcribed ^{32}P-radiolabeled antisense RNA probes were prepared from cDNA templates using Strip-EZ RNA T7 kit (Ambion) or MAXIscript T7 kit (Ambion). Hybridization and washes were carried out at 68 °C using NorthernMax wash buffers (Ambion). Hybridized membranes were exposed overnight to a phosphor screen (Molecular Dynamics) and detected using a Typhoon Scanner (GE Healthcare).

Primers used to make probes are as follows: *lst-1*, prAK102 (5′-ggcttcttcgtcggagaacatg-3′) and prAK103 (5′-TAATACGACTCACTATAGGGAGAgaaccggcacgatcgagttg-3′); *sygl-1*, prHJS143 (5′-CCGCTGAGCAATAACTAGCatgccattccattatccaaaactc-3′) and prHJS144 (5′-TAATACGACTCACTATAGGGctactgcaaataatagctgttgg-3′); *eft-3*, KRN195 (5′-caagtacgcttgggtctc-3′) and KRN196 (5′-TAATACGACTCACTATAGGcctcagagaatggtggctc-3′). Capital letters in prAK103, KRN196, and prHJS144 indicate the T7 promoter sequence used for in vitro transcription. Capital letters in prHJS143 indicate the T7 terminator sequence.

1. Brenner S (1974) The genetics of *Caenorhabditis elegans*. *Genetics* 77(1):71–94.
2. Francis R, Barton MK, Kimble J, Schedl T (1995) *gld-1*, a tumor suppressor gene required for oocyte development in *Caenorhabditis elegans*. *Genetics* 139(2):579–606.
3. Kadyk LC, Kimble J (1998) Genetic regulation of entry into meiosis in *Caenorhabditis elegans*. *Development* 125(10):1803–1813.
4. Singh K, et al. (2011) *C. elegans* Notch signaling regulates adult chemosensory response and larval molting quiescence. *Curr Biol* 21(10):825–834.
5. Sijen T, et al. (2001) On the role of RNA amplification in dsRNA-triggered gene silencing. *Cell* 107(4):465–476.
6. Crittenden SL, et al. (2002) A conserved RNA-binding protein controls germline stem cells in *Caenorhabditis elegans*. *Nature* 417(6889):660–663.
7. Lamont LB, Crittenden SL, Bernstein D, Wickens M, Kimble J (2004) FBF-1 and FBF-2 regulate the size of the mitotic region in the *C. elegans* germline. *Dev Cell* 7(5):697–707.
8. Austin J, Kimble J (1987) *glp-1* is required in the germ line for regulation of the decision between mitosis and meiosis in C. elegans. *Cell* 51(4):589–599.
9. Berry LW, Westlund B, Schedl T (1997) Germ-line tumor formation caused by activation of *glp-1*, a *Caenorhabditis elegans* member of the *Notch* family of receptors. *Development* 124(4):925–936.
10. Berset T, Hoier EF, Battu G, Canevascini S, Hajnal A (2001) Notch inhibition of RAS signaling through MAP kinase phosphatase LIP-1 during *C. elegans* vulval development. *Science* 291(5506):1055–1058.
11. Kennedy S, Wang D, Ruvkun G (2004) A conserved siRNA-degrading RNase negatively regulates RNA interference in *C. elegans*. *Nature* 427(6975):645–649.
12. Siegfried KR, Kimble J (2002) POP-1 controls axis formation during early gonadogenesis in *C. elegans*. *Development* 129(2):443–453.
13. Byrd DT, Knobel K, Affeldt K, Crittenden SL, Kimble J (2014) A DTC niche plexus surrounds the germline stem cell pool in *Caenorhabditis elegans*. *PLoS ONE*, in press.
14. Lin R (2003) A gain-of-function mutation in *oma-1*, a *C. elegans* gene required for oocyte maturation, results in delayed degradation of maternal proteins and embryonic lethality. *Dev Biol* 258(1):226–239.
15. Lee M-H, Hook B, Lamont LB, Wickens M, Kimble J (2006) LIP-1 phosphatase controls the extent of germline proliferation in *Caenorhabditis elegans*. *EMBO J* 25(1):88–96.
16. Ward S, Roberts TM, Strome S, Pavalko FM, Hogan E (1986) Monoclonal antibodies that recognize a polypeptide antigenic determinant shared by multiple *Caenorhabditis elegans* sperm-specific proteins. *J Cell Biol* 102(5):1778–1786.
17. Hadwiger G, Dour S, Arur S, Fox P, Nonet ML (2010) A monoclonal antibody toolkit for *C. elegans*. *PLoS ONE* 5(4):e10161.
18. Zetka MC, Kawasaki I, Strome S, Müller F (1999) Synapsis and chiasma formation in *Caenorhabditis elegans* require HIM-3, a meiotic chromosome core component that functions in chromosome segregation. *Genes Dev* 13(17):2258–2270.
19. Kawasaki I, et al. (1998) PGL-1, a predicted RNA-binding component of germ granules, is essential for fertility in *C. elegans*. *Cell* 94(5):635–645.
20. Duerr JS (2006) Immunohistochemistry. *WormBook* (The *C. elegans* Research Community). Available at: www.wormbook.org.
21. Lee M-H, Schedl T (2006) RNA in situ hybridization of dissected gonads. *WormBook* (The *C. elegans* Research Community). Available at: www.wormbook.org.
22. Merritt C, Rasoloson D, Ko D, Seydoux G (2008) 3′ UTRs are the primary regulators of gene expression in the *C. elegans* germline. *Curr Biol* 18(19):1476–1482.
23. Frøkjaer-Jensen C, et al. (2008) Single-copy insertion of transgenes in *Caenorhabditis elegans*. *Nat Genet* 40(11):1375–1383.
24. Shirayama M, et al. (2012) piRNAs initiate an epigenetic memory of nonself RNA in the *C. elegans* germline. *Cell* 150(1):65–77.

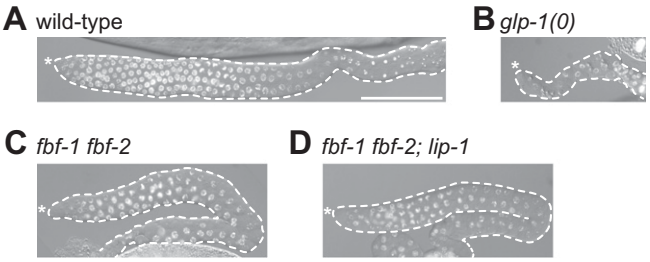

E

Genotype	Total # GCs in adult	Mitotic Zone?	Sperm only?	Reference
wild-type	~2000	+	–	(1)
glp-1(null)	4-8	–	+	(2)
glp-1(ts) L1 shift	4-8	–	+	(2)
glp-1(ts) L4/A shift	>100	–	+	(2)
fbf-1 fbf-2	>100	–	+	(3)
fbf-2; lip-1	>100	+	–	(this work)
fbf-1 fbf-2; lip-1	>100	–	+	(this work)

Fig. S1. Known GLP-1/Notch target genes do not mimic *glp-1*. (*A*–*D*) Gonads dissected from L4 hermaphrodites (overlay of DIC and DAPI stained images). Asterisk marks distal end, where the GSC niche resides; dotted line demarcates germ-line tissue. The scale bar in *A* also applies to the images in *B*, *C*, and *D* and equals 100 μm. (*A*) Wild-type GSCs generate normal germ cell number. (*B*) *glp-1* null mutant GSCs generate only four to eight germ cells, which differentiate as sperm (2). (*C*) *fbf-1 fbf-2* double-mutant GSCs generate germ cells normally during larval development, but lose their capacity for self-renewal in late L4 larvae and adults (3). (*D*) *fbf-1 fbf-2; lip-1* triple mutants lack the only two previously known GLP-1/Notch target genes affecting germ-line proliferation (*fbf-2* and *lip-1*); their GSC self-renewal capacity is restricted to larval development as in *fbf-1 fbf-2* double mutants (this work). (*E*) Table summarizing mutant effects on GSC self-renewal.

1. Crittenden SL, Leonhard KA, Byrd DT, Kimble J (2006) Cellular analyses of the mitotic region in the *Caenorhabditis elegans* adult germ line. *Mol Biol Cell* 17(7):3051–3061.
2. Austin J, Kimble J (1987) *glp-1* is required in the germ line for regulation of the decision between mitosis and meiosis in C. elegans. *Cell* 51(4):589–599.
3. Crittenden SL, et al. (2002) A conserved RNA-binding protein controls germline stem cells in *Caenorhabditis elegans*. *Nature* 417(6889):660–663.

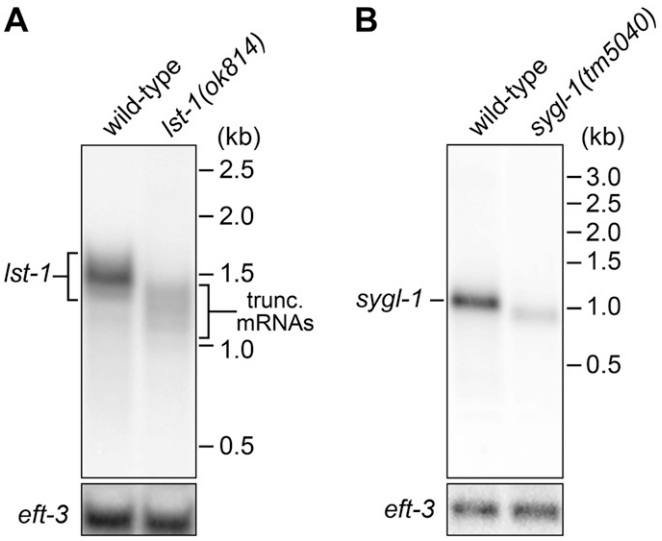

Fig. S2. Northern analysis of *lst-1* and *sygl-1* transcripts. See Fig. 1*C* for site of deletions and extent of exons targeted by probes. (*A*) Northern blot of *lst-1* mRNA in wild-type and *lst-1(ok814)* mutant. Wild-type animals produce a predominant ~1.5-kb mRNA, consistent in size to the shorter *lst-1S* isoform. RNA-seq data also indicate that the *lst-1S* is more abundant than the *lst-1L* isoform (1). *lst-1* single mutants lack that band and instead produce smaller, truncated mRNAs of ~1.0–1.5 kb in length. (*B*) Northern blot of *sygl-1* mRNA in wild-type and *sygl-1(tm5040)* mutant. Wild-type animals produce a single ~1.0-kb mRNA. *sygl-1(tm5040)* single mutants produce a truncated mRNA.

1. Gerstein MB, et al.; modENCODE Consortium (2010) Integrative analysis of the *Caenorhabditis elegans* genome by the modENCODE project. *Science* 330(6012):1775–1787.

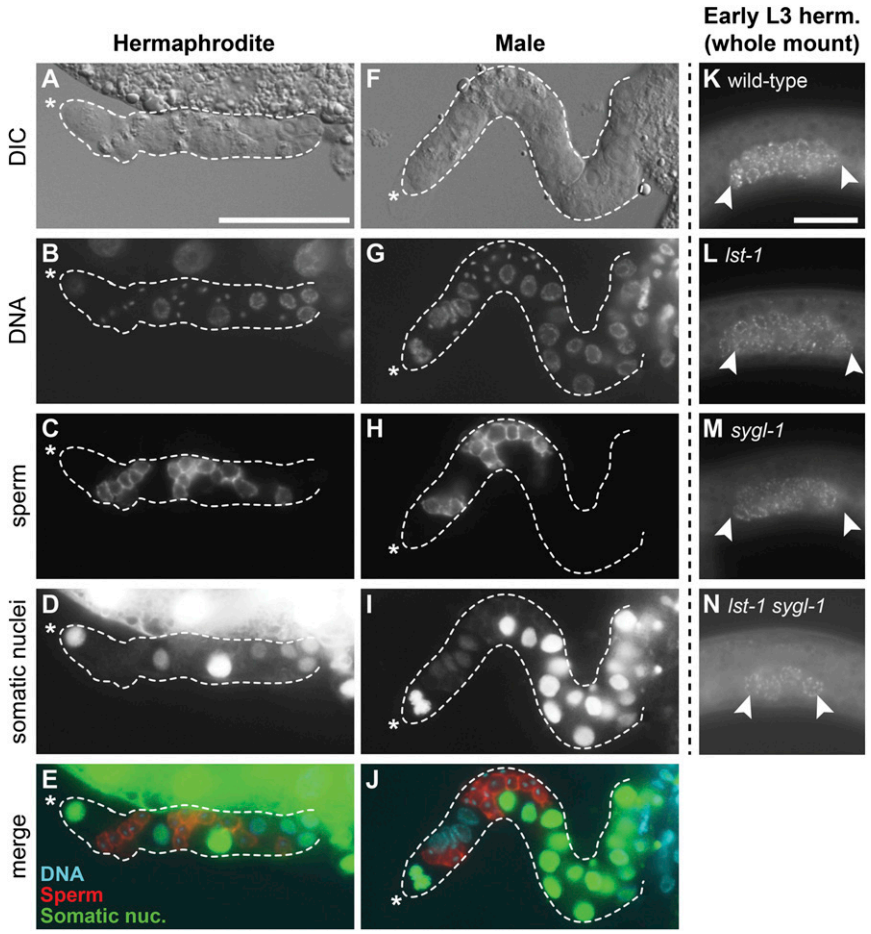

Fig. S3. *lst-1 sygl-1* double mutants do not maintain GSCs in either sex. (*A–J*) Gonads dissected from early L4 *lst-1 sygl-1* hermaphrodite (*A–E*) and *lst-1 sygl-1* male (*F–J*). Each hermaphrodite possesses two gonadal arms, whereas males possess only one gonadal arm. The hermaphrodite arm shown in *A–E* is representative with an average of 14 ± 3 mature sperm derived from three to four premeiotic germ cells ($n = 9$). The male gonad shown in *F–J* is representative with an average of 22 ± 2 sperm derived from five to six premeiotic germ cells ($n = 15$). Asterisk marks distal end; dotted line demarcates entire germ-line tissue plus the DTC niche and a few additional somatic cells more proximally. The scale bar in *A* also applies to the images in *B–J* and equals 50 μm. (*A* and *F*) Full extruded gonadal arm visualized with DIC. (*B* and *G*) Same arm stained with DAPI to show all nuclei. (*C* and *H*) Same arm stained with sperm-specific marker SP56. (*D* and *I*) same arm stained with a marker for somatic cells (complex integrated array harboring GFP driven by *sur-5* promoter). (*E* and *J*) Merge of *A–D* and *F–I*, respectively. (*K–N*) Shown are representative images of early L3 hermaphrodite larvae before spermatogenesis whole mount stained using antibodies against PGL-1, which mark premeiotic germ cells (19). White arrowheads mark ends of the region containing PGL-1–positive cells. The scale bar in *K* also applies to *L–N* and equals 25 μm. Wild type (*K*), *lst-1(ok814)* homozygotes (*L*), *sygl-1(tm5040)* homozygotes (*M*), and *lst-1 sygl-1* homozygous double mutants (*N*). Germ cell numbers are reported in Fig. 2*F*.

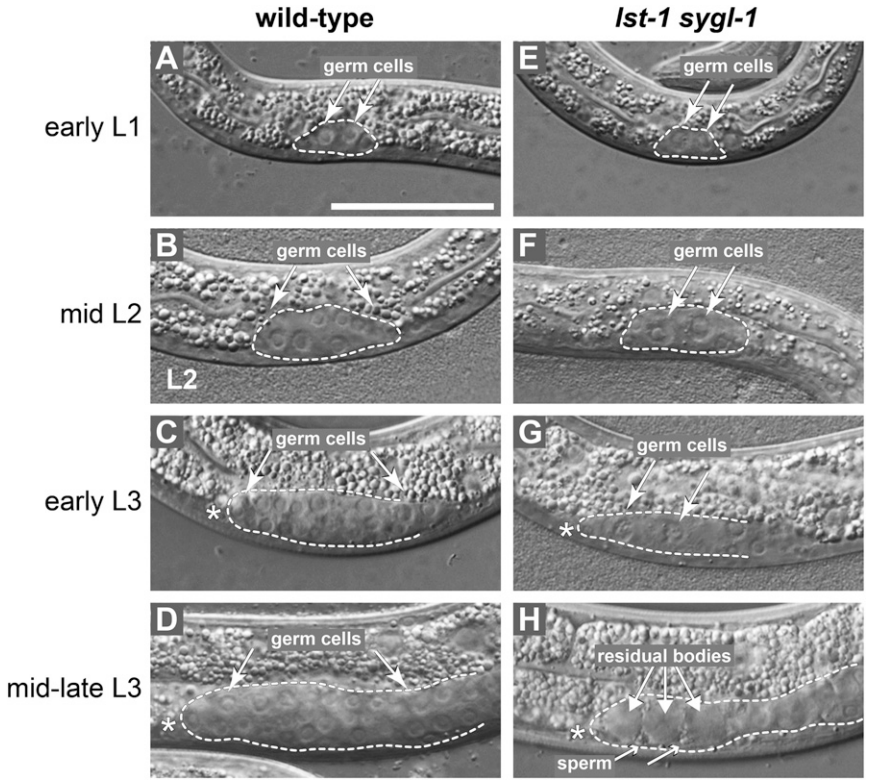

Fig. S4. Germ cells undergo spermatogenesis precociously in *lst-1 sygl-1* double mutants. (*A–H*) Nomarski micrographs of larval hermaphrodites from L1 (*A* and *E*) to L3 (*D* and *H*). The dotted line surrounds entire gonad in early L1 and mid-L2 images and surrounds one gonadal arm in L3 images. The scale bar in *A* equals 50 μm and also applies to *B–H*. (*A–D*) Wild-type germ cells remain undifferentiated during first three larval stages. Arrows indicate extent of germ-line proliferation at individual stages. (*E–H*) Germ cells in *lst-1 sygl-1* double mutants are far fewer in number than wild type and complete both spermatogenic meiotic divisions precociously (by mid-late L3) to generate small compact sperm and large residual bodies which contain much of the cytoplasm of primary spermatocytes. Only three residual bodies are seen, which corresponds well in number with the ~three to four premeiotic germ cells counted per *lst-1 sygl-1* gonadal arm (Fig. 2*F* and Fig. S3). Asterisk marks distal end.

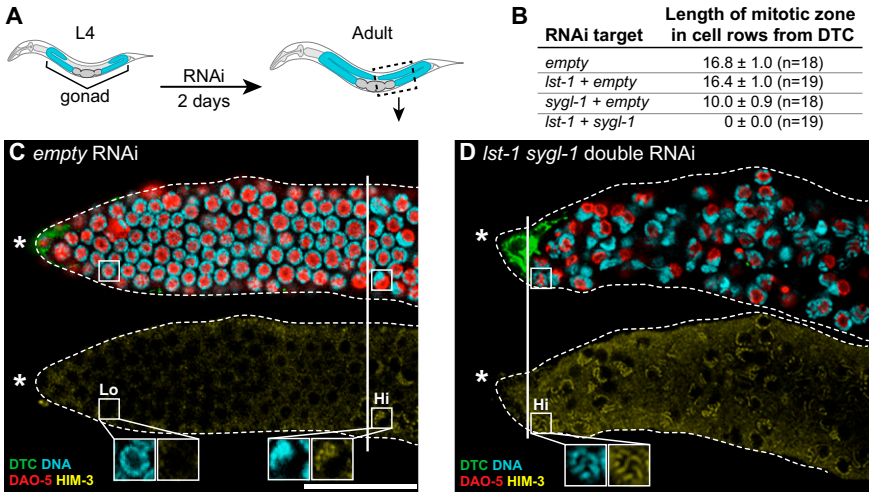

Fig. S5. *lst-1* and *sygl-1* function redundantly to promote GSC self-renewal in adults. (*A*) Experimental regimen. Wild-type late L4 larvae were treated with RNAi for 48 h and scored as adults. RNAi used either empty vector alone, empty vector plus *lst-1*, empty vector plus *sygl-1*, or *lst-1* plus *sygl-1*. (*B*) Mitotic zones were measured in number of germ cell diameters from distal end; the region was scored using morphology of DAPI-stained chromosomes to detect the first meiotic prophase nuclei and also by the extent of staining with anti–REC-8 antibodies, which corresponds well to the mitotic zone (1). Averages are given with the 95% confidence interval. RNAi depletion of only *lst-1* or *sygl-1* left the mitotic zone intact, but RNAi depletion of both *lst-1* and *sygl-1* abolished the mitotic zone. (*C* and *D*) Empty RNAi germ lines possess a mitotic zone, but *lst-1 sygl-1* double RNAi do not. Shown are representative confocal images of extruded gonads from animals treated either with empty RNAi or RNAi directed against both *lst-1* and *sygl-1* stained with antibodies against HIM-3 (yellow). A low level of nonchromosomal HIM-3 is typical of nuclei in the mitotic cell cycle (e.g., cell marked "Lo"), whereas a high level of chromosomal HIM-3 is typical of nuclei in meiotic prophase (e.g., cell marked "Hi"). Representative nuclei are shown in 2× magnified insets to more clearly visualize staining as nonchromosomal or chromosomal. Asterisk denotes distal end; dotted line delimits gonadal arm. The strain used for these images included a transgene with GFP expressed in the DTC at the distal end of the gonad. Antibodies against nucleolar marker DAO-5 helped distinguish germ cells in the mitotic cell cycle from those in early meiotic prophase: DAPI staining surrounds DAO-5 nucleolar staining in most germ cells in the mitotic cell cycle, whereas in early meiotic prophase where chromosomes have begun to pair (2), DAPI is asymmetrically localized relative to DAO-5 and typically forms a crescent. The scale bar in *C* equals 25 μm and also applies to *D*. (*C*) Confirmation that control RNAi germ lines possess a mitotic zone. As germ cells progress proximally from the distal end (asterisk), the distal nuclei possess low nonchromosomal HIM-3 staining; the first nuclei with high chromosomal HIM-3 staining correspond to the onset of meiotic prophase as seen by DAPI (solid white line). (*D*) *lst-1 sygl-1* double RNAi germ lines lack a mitotic zone. Meiotic prophase nuclei and high chromosomal HIM-3 (see cell marked "Hi") extend to the distal end (solid white line).

1. Hansen D, Hubbard EJA, Schedl T (2004) Multi-pathway control of the proliferation versus meiotic development decision in the *Caenorhabditis elegans* germline. *Dev Biol* 268(2):342–357.
2. Dernburg AF, et al. (1998) Meiotic recombination in *C. elegans* initiates by a conserved mechanism and is dispensable for homologous chromosome synapsis. *Cell* 94(3):387–398.

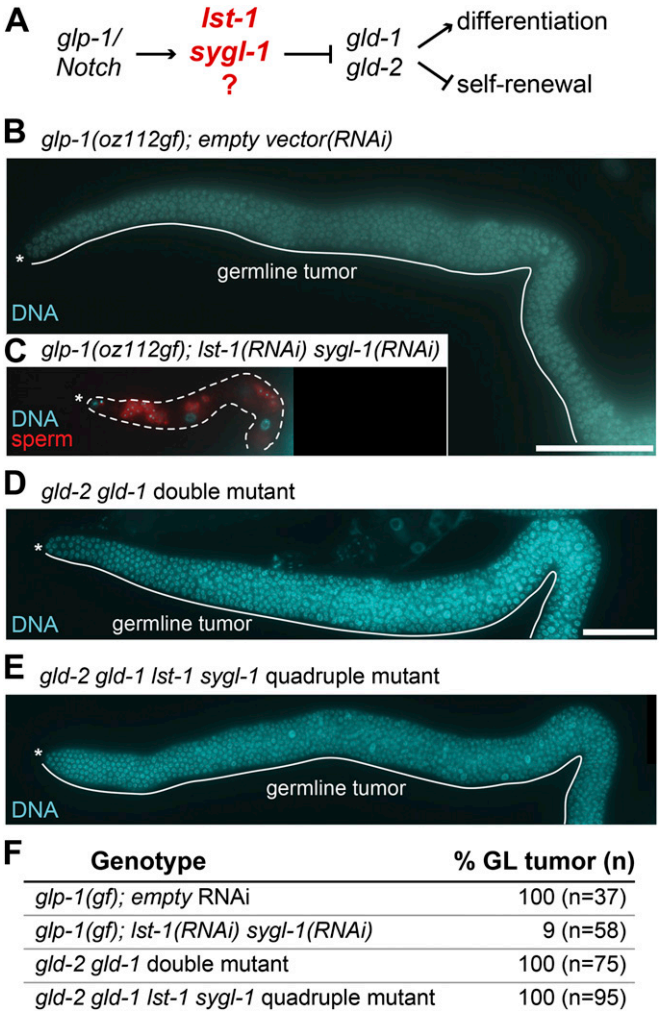

F

Genotype	% GL tumor (n)
glp-1(gf); empty RNAi	100 (n=37)
glp-1(gf); lst-1(RNAi) sygl-1(RNAi)	9 (n=58)
gld-2 gld-1 double mutant	100 (n=75)
gld-2 gld-1 lst-1 sygl-1 quadruple mutant	100 (n=95)

Fig. S6. Genetic epistasis experiments begin to place *lst-1* and *sygl-1* into GSC regulatory pathway. (*A*) Simplified genetic pathway governing GSC self-renewal or differentiation. If *lst-1* and *sygl-1* are critical GLP-1/Notch targets for GSC self-renewal, they are expected to behave genetically as downstream of *glp-1/Notch* signaling and upstream of *gld-2 gld-1*, which promote differentiation. Arrows denote activation, bars repression. (*B–E*) Representative images of gonads dissected from adult hermaphrodites. Asterisk marks distal end. DAPI staining (blue) shows nuclei. The scale bars equal 100 μm, with the scale bar in *B* also applying to *C*, and the scale bar in *D* also applying *E*. (*B*) All *glp-1(oz112gf)* animals treated with control RNAi produced large germ-line tumors (Tum). (*C*) The vast majority of *glp-1(oz112gf)* animals treated with *lst-1 sygl-1* double RNAi had tiny germ lines with only differentiated sperm (red); therefore, the *lst-1 sygl-1* Glp defect is epistatic to the *glp-1(oz112gf)* Tum defect. (*D*) All *gld-2 gld-1* double-mutant germ lines were Tum. (*E*) All *gld-2 gld-1 lst-1 sygl-1* quadruple mutant germ lines were also Tum; therefore, the *gld-2 gld-1* Tum defect is epistatic to the *lst-1 sygl-1* Glp defect. (*F*) Summary of epistasis data.

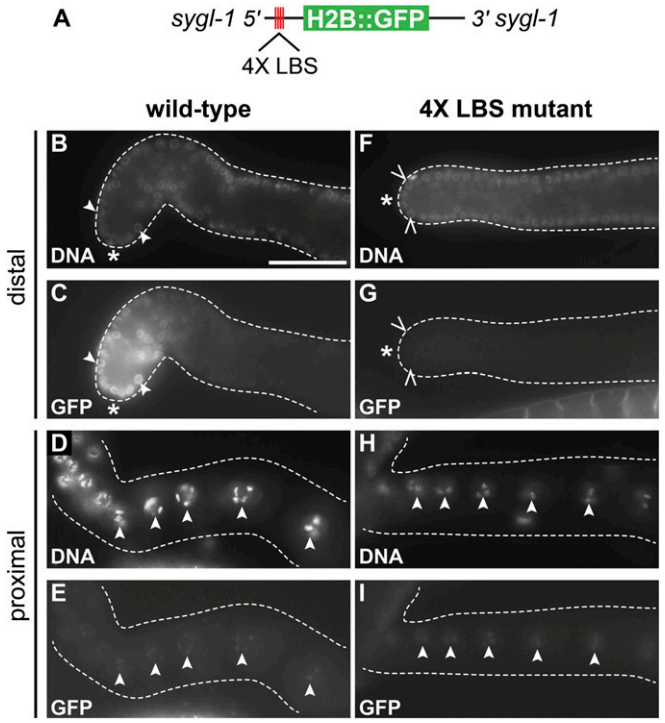

Fig. S7. *sygl-1* reporter transgenes are not silenced in the germ line. (*A*) Diagram of reporter using wild-type *sygl-1* promoter to control H2B::GFP expression. The cluster of four LAG-1 binding sites (LBS) is indicated. (*B–I*) Shown are compound fluorescence images of dissected unfixed germ lines expressing either the wild-type *sygl-1* reporter or the 4× LBS mutant version. *B–E* show images of the same gonad, as do *F–I*. Samples were scored for the presence of the nuclear H2B::GFP reporter and also stained with Hoechst 33342 to visualize DNA. Arrowheads mark examples of H2B::GFP-positive nuclei; carets mark examples of H2B::GFP-negative nuclei. Asterisk marks distal end of the germ line; dotted lines show germ-line boundaries. The scale bar in (*B*) also applies to *C–I* and equals 50 μm. (*B–E*) In the distal gonad, expression of the wild-type *sygl-1* reporter is limited to nuclei of the most distal germ cells (*C*); in the proximal gonad, expression of the wild-type *sygl-1* reporter is observed faintly in oocyte nuclei. All germ lines with detectable GFP expressed the transgene in both distal and proximal nuclei ($n = 45$). (*F–I*) The 4× LBS mutant *sygl-1* reporter was not expressed in distal-most germ cells (*G*) but was detectable in proximal oocyte nuclei (*I*). For this mutant promoter, expression was limited to oocytes in all germ lines ($n = 46$). Therefore, although transgene expression was absent from distal germ cells, it was detectable in oocytes, and hence it was not silenced broadly in the germ line.

Table S1. Genes common to predicted Notch targets and putative FBF-1 targets

Gene	Molecular function	Human homolog	*C. elegans* germ line expressed?
sygl-1	Novel	None	Yes (1, 2)
lst-1	Novel	None	Yes (1, 2)
ima-3	Importin α nuclear transport factor	Importin subunit α-4	Yes (2, 3)
lin-45	RAF protein kinase	*RAF*	Yes (1)
lst-4	Sorting nexin	Sorting nexin-33	Yes (1, 2)
mau-2	Chromatid cohesion factor	*MAU2*	Yes (1, 2)
nhr-46	Nuclear hormone receptor	Hepatocyte nuclear factor 4-α	Yes (1)
npp-13	Nuclear pore complex protein	*NUP93*	Yes (1)
smg-6	Telomerase interacting protein	*EST1A*	Yes (1)
tag-341	Rho GTPase-activating protein	Rho GTPase-activating protein 29	Yes (1)
ulp-2	Ubiquitin-like protease	Sentrin-specific protease 6	Yes (1, 2)
vha-7	Vacuolar H ATPase subunit	Lysosomal ATPase V0 subunit a1	Yes (1)
yif-1	Protein transport	*YIF1A*	Unknown
F57G12.1	Novel	None	Yes (1)
Y60A3A.8	Novel	None	Unknown

1. The Nematode Expression Pattern DataBase (NEXTDB) Release v. 4.0. Available at http://nematode.lab.nig.ac.jp/db2/index.php. Accessed August 2013.
2. Reinke V, Gil IS, Ward S, Kazmer K (2004) Genome-wide germline-enriched and sex-biased profiles in *Caenorhabditis elegans*. *Development* 131(2):311–323.
3. Geles KG, Adam SA (2001). Germline and developmental roles of the nuclear transport factor importin α3 in *C. elegans*. *Development* 128(10):1817–1830.

Table S2. Single and double RNAi to seek Glp phenotype

	Single RNAi in wild type		Double RNAi with *sygl-1**		Single RNAi in *lst-1* mutant		Single RNAi in *sygl-1* mutant	
RNAi target gene	fertile	Glp	fertile	Glp	fertile	Glp	fertile	Glp
Empty[†,‡]	+	–	+	–	+	–	+	–
sygl-1[†]	+	–	NA	NA	–	+	NA	NA
lst-1[†]	+	–	–	+	NA	NA	–	+
ima-3[†]	–	–	–	–	–	–	ND	ND
lin-45[†]	+	–	+	–	+	–	ND	ND
lst-4[†]	+	–	+	–	+	–	ND	ND
mau-2[†]	+	–	+	–	+	–	ND	ND
nhr-46[†]	+	–	+	–	+	–	ND	ND
npp-13[†]	–	–	ND	ND	–	–	–	–
smg-6[‡]	+	–	ND	ND	+	–	+	–
tag-341[†]	+	–	+	–	+	–	ND	ND
ulp-2[‡]	+	–	ND	ND	+	–	+	–
vha-7[†]	+	–	+	–	+	–	ND	ND
yif-1[†]	+	–	+	–	+	–	ND	ND
F57G12.1[†]	+	–	+	–	+	–	ND	ND
Y60A3A.8[‡]	+	–	ND	ND	+	–	+	–

Glp phenotype was scored for any dramatic effect on germ-line proliferation. +, positive; –, negative; NA, not applicable; ND, no data.
*Used RNAi hypersensitive mutant *eri-1(mg366)*.
[†]L1 RNAi feeding, score treated animals as young adults.
[‡]L4 RNAi feeding, score next generation as young adults.

Table S3. Deletion mutants and RNAi confirm Glp effect

Genotype*	RNAi target(s)	% Glp	*n*
Wild-type	Empty vector	0	259
Wild-type	*lst-1*	0	86
Wild-type	*sygl-1*	0	154
Wild-type	*lst-1* and *sygl-1*	89	112
lst-1 deletion	Empty vector	0	167
lst-1 deletion	*sygl-1*	100	124
sygl-1 deletion	Empty vector	0	61
sygl-1 deletion	*lst-1*	100	51
rrf-1	Empty vector	0	47
rrf-1	*lst-1*	0	50
rrf-1	*sygl-1*	0	52
rrf-1	*lst-1* and *sygl-1*	98	65

*Alleles: *lst-1(ok814)*, *sygl-1(tm5040)*, and *rrf-1(pk1417)*.